Effect of filler loading on the polymorphs of calcium carbonate crystallization of chitin reinforced polymer

Michael Ikpi Ofem (PhD), Muneer Umar (PhD) , Musa Muhammed (M.Eng)

Abstract: Crystals were precipitated by evaporation casting method within a very short time of 5 minutes at 30°C. The crystals were grown in chitin whiskers (CHW), Poly (acrylic acid) (PAA) and CHW/PAA composites. The volume fraction for calcite, vaterite and aragonite were respectively 0.65, 0.25 and 0.10. The calcite and aragonite volume fractions decrease in favour of vaterite as PAA increases up to 11%cw. At 3%cw aragonite polymorph growth was favoured to the detriment of calcite. SEM images in the absence of PAA and CHW, showed rhombohedral calcites were observed while rod-like aragonite polymorphs were seen when only PAA was used as template. In the presence of only CHW, a morphological mixture of ellipsoidal and disc shape with traces of rhombohedral aggregate calcite dominated the features. In the presence of both PAA and CHW, the rhombohedral shape showed roughness with irregular faces while the vaterite polymorph continued to agglomerate with the observation of porosity at higher CHW content.

Key words: Calcium carbonate, chitin, filler loading, polymorphs, volume fractions, whiskers,

1. INTRODUCTION

Biomineralization is a process in which living organisms produce inorganic/organic hybrids. The production of this hybrid under different conditions has received attention in recent years. The essence of producing this biomineral is to have a complex but environmentally friendly morphology and as well as better mechanical properties. However, the understanding of these hybrids' development processes is still a subject of research. It has been reported that the exoskeleton of the crayfish is composed of about 50:50wt% of $CaCO_3$ and organic macromolecules such as chitin and proteins. Calcium carbonate polymorphs (calcite, vaterite or aragonite) are some of the mineral phases formed when an insoluble polymer with the help of a soluble agent of polymeric anions is induced on a substrate [1], [2]. The production of these polymorphs might be influenced by the conditions of precipitation and the presence of impurities in an aqueous solution. Of the three polymorphs, calcite is the most thermodynamically stable under ambient conditions while the least stable is vaterite. A variety of $CaCO_3$ crystal/chitin or chitosan based hybrid materials have been reported. These reports have shown the formation of calcite on insoluble polysaccharides (chitin and chitosan) and soluble additives like PAA [1], [3], [4], [5], [6]. The interaction of these polyanions and chitin/chitosan provides a nucleation site for the formation of calcium carbonate polymorphs.

Calcium carbonate was precipitated on three insoluble polymer matrices namely chitin, cellulose and chitosan [7]. Their derivatives (OH and NH_2 were synthesized by the acetylation of hydroxyl groups following the *N*-phthaloylation of the amino group of chitosan and the acetylation of chitin respectively to prevent proton donation in the presence of PAA. The crystal growth resulted in the formation of $CaCO_3$ thin-film crystals of about 0.8μm in thickness. The crystallite size as measured by X-ray was 30nm. No precipitation was observed for the crystallization on the insoluble polymer matrices derivatives possessing no proton-donating group (cellulose and chitin), even in the presence of PAA, but rhombohedral calcite crystals were obtained in the absence of the acidic polymer PAA. Thin films grown on chitosan consisted of mainly vaterite and those of cellulose and chitin consist of only calcite in the absence of PAA, while those grown on chitosan mainly consist of vaterite in the presence of the PAA. Polymorphs formed on the thin films developed on chitin and cellulose was independent of the concentration of PAA, where as those of chitosan were dependent. A higher molecular weight of PAA led to less stable polymorphs.

Oriented chitin films as templates were used for $CaCO_3$ crystallization in the presence of poly(acrylic acid), (PAA).[7] At about 10 hours after immerging the films in the crystallization solution at a temperature of 5 °C small rods of about 8 µm in length of $CaCO_3$ crystals were observed. The rod-like $CaCO_3$ crystals increase in length to 80µm after 50 hours of immersion. The diameter of the rod was between 10 and 30µm. At 30°C similar crystallization behaviour was observed.

The diffusion method of $CaCO_3$ crystallisation on CHW or chitosan reported by most authors takes hours or days for $CaCO_3$ growth on the substrate. There is limited literature on the growth of $CaCO_3$ by evaporation method and within

a very short period. Therefore, the need to use a new method of calcium carbonate crystallisation with a very short time span necessities the evaporation method. Here we report the formation of different calcium polymorphs at higher filler loading of chitin whiskers using the evaporation method of crystallisation at a very short time.

2.0 Experimental methodology

2.1 Preparation of Chitin whiskers (CHW)/PAA/$CaCO_3$ composites.

Shrimp Chitin, Poly (acrylic acid) (PAA) and all chemicals were purchased from Sigma Aldrich, UK. A 0.2M of K_2CO_3 and 0.2M of $CaCl_2$ at a ratio of 1:1 by volume were mixed in a beaker at 30 °C for 5 minutes while stirring. The solid precipitate, obtained immediately after mixing the two solutions, was collected by filtrations. The collected precipitate was rinsed three times with deionised water. Finally, the $CaCO_3$ precipitates were dried in an oven at 100 °C for 1 hour, resulting in finely grained powders. 0.3wt % chitin whiskers(CHW) were prepared as reported elsewhere[8], [9], [10]. To incorporate $CaCO_3$ into the composite, 5ml of K_2CO_3 and 5ml of $CaCl_2$ were mixed with various weight fractions of CHW and PAA. The CHW/PAA/$CaCO_3$ in the beaker was heated at 30°C for 5 minutes. The CHW/PAA/$CaCO_3$ solution was poured in a plastic petri dish and allowed to dry in a fume hood and later in the oven. The final volume before drying was maintained at 60 ml. The weight fractions of CHW were 0.73, 0.42, 0.23, 0.11 and 0.03.

2.2 Characterisation of Composites

XRD measurements of films were carried out using X'Pert PW3710MPD, Philips with Cu Kα radiation (λ=1.54 Å) with an acceleration voltage of 40KV and current of 30mA. A range of 2θ = 10-60^0 was scanned at a continuous scan step size of 0.02 and step time of 5s per scan. Renishaw system 1000 spectrometer was used to collect the Raman spectra, using a 785 nm near infrared laser. An FEM-SEM XL-30 scanning electron microscope operating at a voltage of 10 kV was used to obtain the morphology of films.

3.0 Result and discussion

3.1Raman spectra characterisations

The Raman spectra of the samples prepared at 30 °C in the absence of PAA or CHW are presented in Figure 1A. The yield of $CaCO_3$ was 15%. The observed bands were assigned based on values from literature [1], [11], [12], [13], [14]. In the absence of PAA and chitin, calcite bands and one band of vaterite were observed. Strong calcite bands at 154 and 281cm^{-1} (translational lattice modes), 711 cm^{-1} (ν_4 -in plane bending), 1087 cm^{-1} (ν_1- asymmetric stretching) and 1437 cm^{-1} (ν_3 -asymmetric stretching) were observed. Another peak at 1750 cm^{-1} which has been interpreted as the combination of ν_4-in plane bending and ν_1-asymmetric stretching was also observed. Only vaterite was observed at 874 cm^{-1} (ν_2 -out of plane bending mode). Figure 1B presents the crystallization of calcium carbonate in the presence of chitin while figure 1C is the crystallization of calcium carbonate in the presence of PAA. The polymorph of $CaCO_3$/PAA is a combination of phases; calcite, aragonite and vaterite. Three peaks namely: 148, 274 cm^{-1} (translational lattice modes) and 707 cm^{-1} (ν_4 -in plane bending) for aragonite. For calcite, 1086 cm^{-1} (ν_1-asymmetric stretching) and 1437 cm^{-1} earlier observed for the calcite crystalline phase moved to 1433 cm^{-1} (ν_3 -asymmetric stretching). 873cm^{-1} (ν_2 -out of plane bending mode) and 1451 cm^{-1} (ν_3-asymmetric stretching) for vaterite which can equally be called amorphous $CaCO_3$ (ACC) [15]. The peak at 1330 cm^{-1} is CH_2 deformation of PAA, the one at 1660 cm^{-1}, corresponds to asymmetric C=O stretching of the carboxylate anions in the PAA matrix. Two polymorphs were observed for $CaCO_3$/CHW crystallisation. These are 153 cm^{-1} and 280 cm^{-1} (translational lattice mode), 712 cm^{-1} (ν_4 -in plane bending) and 1086 cm^{-1} (ν_1- asymmetric stretching) for calcite while 872 cm^{-1} (ν_2 -out of plane bending mode) for vaterite was observed. Two other peaks 1334 and 1558 cm^{-1} are assigned to the CH_2 and NH deformations of chitin respectively.

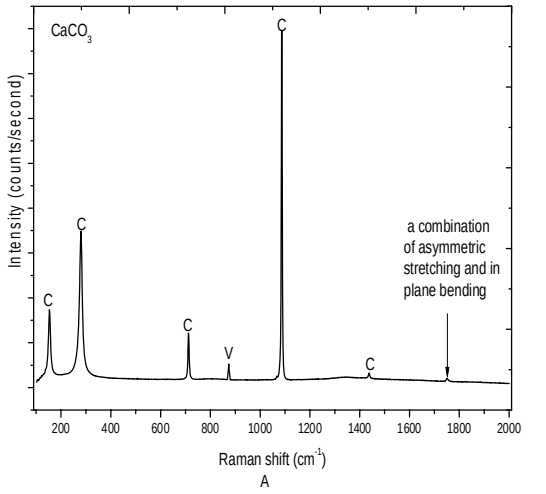

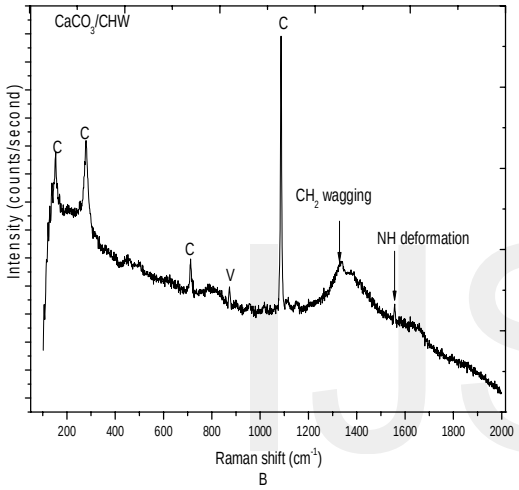

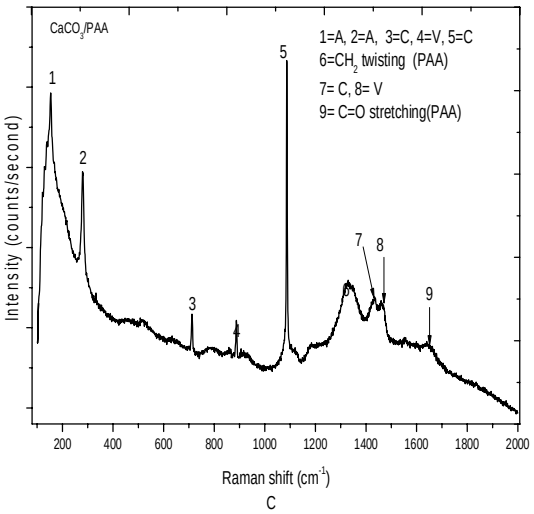

Figure 1 - Raman spectra of $CaCO_3$ crystallisation: (A) in the absence of CHW and PAA (b) in the presence of CHW (c) in the presence of PAA. (A=aragonite, C=calcite and V= vaterite)

Figure 2 is the Raman spectra of $CaCO_3$ crystallisation at different CHW loading in the presence of PAA. For all samples all three polymorphs (calcite, vaterite and aragonite) were present. The 1750 cm^{-1} a combination of $\nu_1 + \nu_4$ was observed in all samples which gradually moved to lower wavenumber of 1746 cm^{-1} at 3%cw. 1557 cm^{-1} (NH_2 deformation of amide) shifted to lower wavenumber of 1553 cm^{-1} at lower filler loading. CH_2 deformation of PAA at 1337 cm^{-1} equally moved to lower wavenumber of 1334 cm^{-1} as PAA increases and CHW decreased. The amorphous vaterite peak at 1461 cm^{-1} (ν_3- asymmetric stretching) remains relatively the same wave number irrespective of the loading. However, 874 cm^{-1} (ν_2- out of plane bending mode) peak moves to 873 cm^{-1} with smaller intensity. At higher filler loading (73%cw and 42%cw) there is an overlap of calcite and vaterite at 1086 and 1090 cm^{-1} (ν_1- asymmetric stretching), this overlap was not observed at lower filler loading. The 153 and 280 cm^{-1} (translational lattice modes) that was observed for calcite gradually moves to 148 and 274 cm^{-1} as CHW content decreased forming an aragonite polymorph. In the same vein 712 cm^{-1} (ν_4 -in-plane bending) and 1086 cm^{-1} (ν_1 - asymmetric stretching) for calcite moved to lower wavenumber of 707 and 1082 cm^{-1} respectively for aragonite. The gradual shift is an indication of preferential growth of aragonite at higher PAA content. It can be seen that the vaterite peaks at 1460 cm^{-1} are in the amorphous stage indicating low pressure during the formation [14].

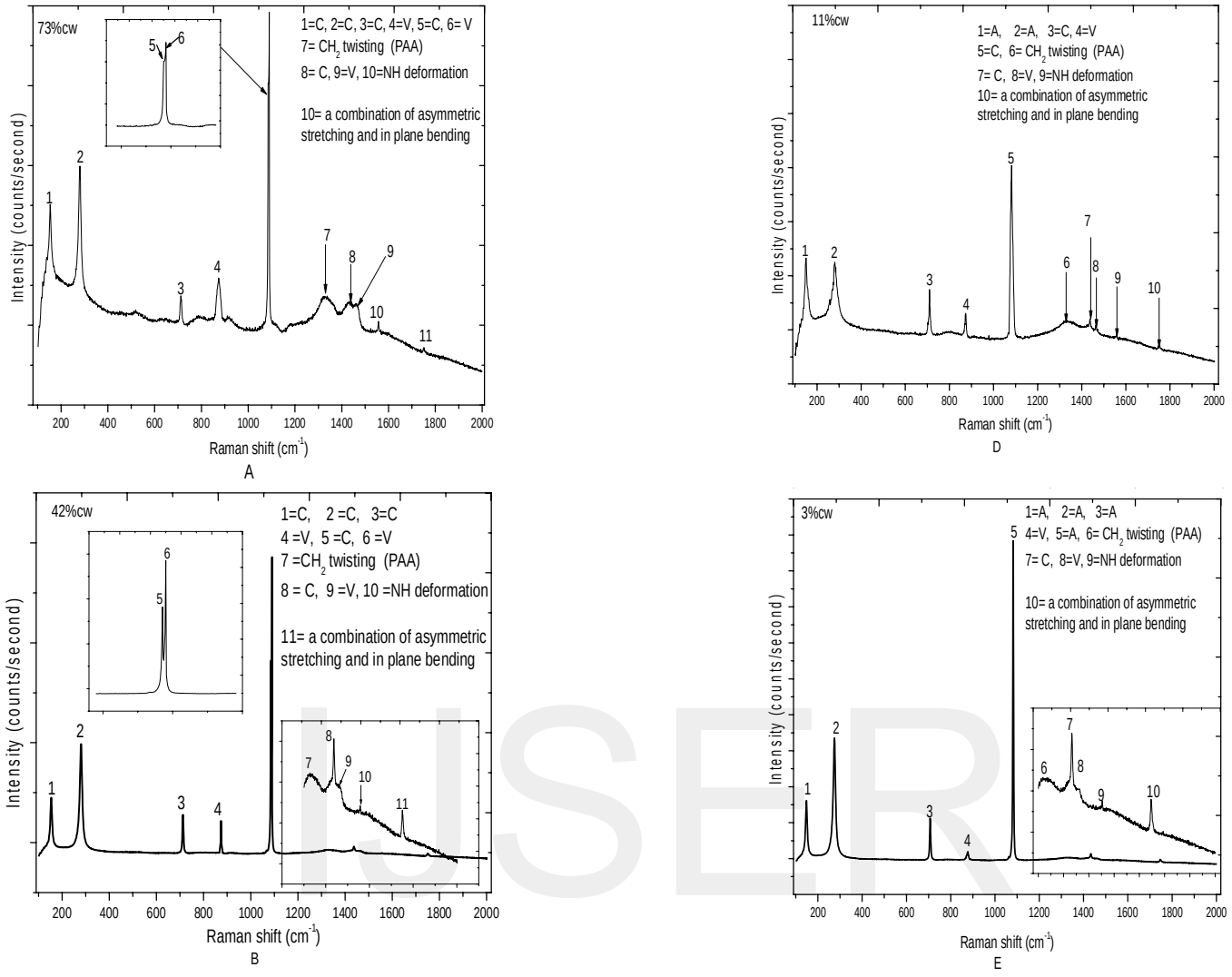

Figure2- Raman spectra of $CaCO_3$ particles synthesized at 30 °C in the presence of PAA (A) 73%cw, (B) 42%cw, (C) 23%cw (D) 11% and (E) 3%cw (A=aragonite, C=Calcite and V=vaterite).

The Raman spectrum of the chitin film showed the characteristic peak of amide I band groups at 1656cm^{-1} and 1622cm^{-1} [16]. In the presence of PAA the band appearing in the spectrum at 1656 cm^{-1},1660 cm^{-1} and 1665 cm^{-1} as filler loading decreases and PAA increases were assigned to the symmetric $-NH^{+2}$ deformation. The band at 1333 cm^{-1} and 1456 cm^{-1} represent the stretching of the –COO– groups. The appearance of these peaks indicates that –COO– and $-NH^{+2}$ coexist on the surface of the chitin membranes in the presence of PAA. The Raman spectrum of PAA/$CaCO_3$ as earlier stated showed the asymmetrical and symmetrical

stretching modes of the –COO– groups appearing at 1660 and 1330 cm^{-1}, respectively. From the Raman spectrum obtained from the CHW in the presence of PAA [16], the band of a symmetric $–NH^{+2}$ deformations appeared at between 1557 and 1553 cm^{-1}, depending on the CHW content and the CH_2-twisting band of PAA appearing between 1337 and 1334cm^{-1}.The shifts in the symmetric $–NH^{+2}$ deformation and CH_2 stretching indicates an electrostatic interaction between PAA and CHW.

From the Raman spectra it could be noticed that at higher PAA content aragonite polymorph formation is favoured. The concentration of PAA in solution has been reported to play a role in $CaCO_3$ precipitation in the presence of chitosan. Excess PAA generates stronger inhibition to grow $CaCO_3$ crystals while low PAA usually lacks action [17]. At low PAA concentration He *et al.,* [18] reported the growth of vaterite on chitosan with 8 % degree of acetylation (DA) while chitosan with 80 % DA favoured the growth of aragonite. At higher concentration the DA did not play any role as the polymorph growth was in favour of vaterite. Wada *et al.,* [19] using different amount of PAA (0.01mg/5ml-4mg/5mg) reported the formation of aragonite and vaterite polymorphs in the presence of chitosan. In the same report the pH value was thought to have contributed to the control of formation of the polymorphs formed. It was reported that at pH of 6.2 only aragonite crystals were formed while at pH 7.8 a combination of aragonite and vaterite were observed. They concluded that the formation and polymorphs generated from $CaCO_3$ depends on the amount of PAA-Ca^{2+} polyelectrolyte complexes formed and the free Ca^{2+} ions left in the $CaCl_2$ solution. The pH in this research was maintained at 7, this may have favoured the appearance of aragonite peaks as PAA increases. The low yield of $CaCO_3$ may have resulted in low PAA-Ca^{2+} polyelectrolyte complexes formation due to the absence of free Ca^{2+} ions thereby resulting to the non appearance of aragonite at higher CHW content (73%cw and 42%cw).

3.2 X-Ray Diffraction characterisation

XRD studies were carried out for the assessment of the composition of different polymorphs of $CaCO_3$ in each sample. The composition of the different polymorphs were analysed using the Joint Committee on Powder Diffraction Standards (*JCPDS*) and other reports from the literature [3], [6], [13], [20], [20], [21]. The XRD pattern of $CaCO_3$ prepared without CHW and PAA is shown in figure 3A while XRD pattern of $CaCO_3$ prepared in the presence of CHW and PAA are presented in figure 3(B) and (C) respectively. For $CaCO_3$ without PAA or CHW strong diffraction peaks around 23.9°(101) for vaterite, 29.4°(104), 31.5°(006), 35.9°(110), 39.4°(113), 47. 5°(018) and 57.4°(221) were assigned for calcite. For $CaCO_3$ growth in the presence of CHW all three polymorphs show strong peaks. These are 29.4° (104), 39.03°(113), 47.3°(018) and 57.4° for calcite, 37.4°(112) and 44.4°(300) for aragonite and vaterite respectively. There is a sharp peak at 22.8°; this peak is assigned to the crystalline peak of chitin. The presence of this peak indicates the confirmation of interaction at the interface between CHW and $CaCO_3$. For $CaCO_3$ in the presence of PAA all three polymorphs are present; with vaterite having the strongest peak at 34.9 °(121) and another at 24.5°(110). Aragonite peaks are 26.3° (111), 33.1°(012), 37.4°(031), 42.8°(220), 45.8°(221), 50.3°(132) and 52.7°(113). Calcite peaks shows presence at 47.5°(018) and 57.3°(122). Contrary to the Raman spectra, no peak for PAA at 2θ≈ 17-19° and at 22° [22], [23], was observed.

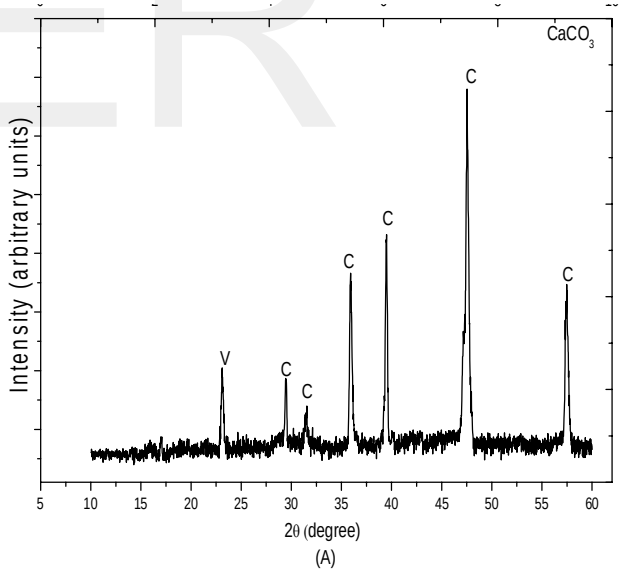

(A)

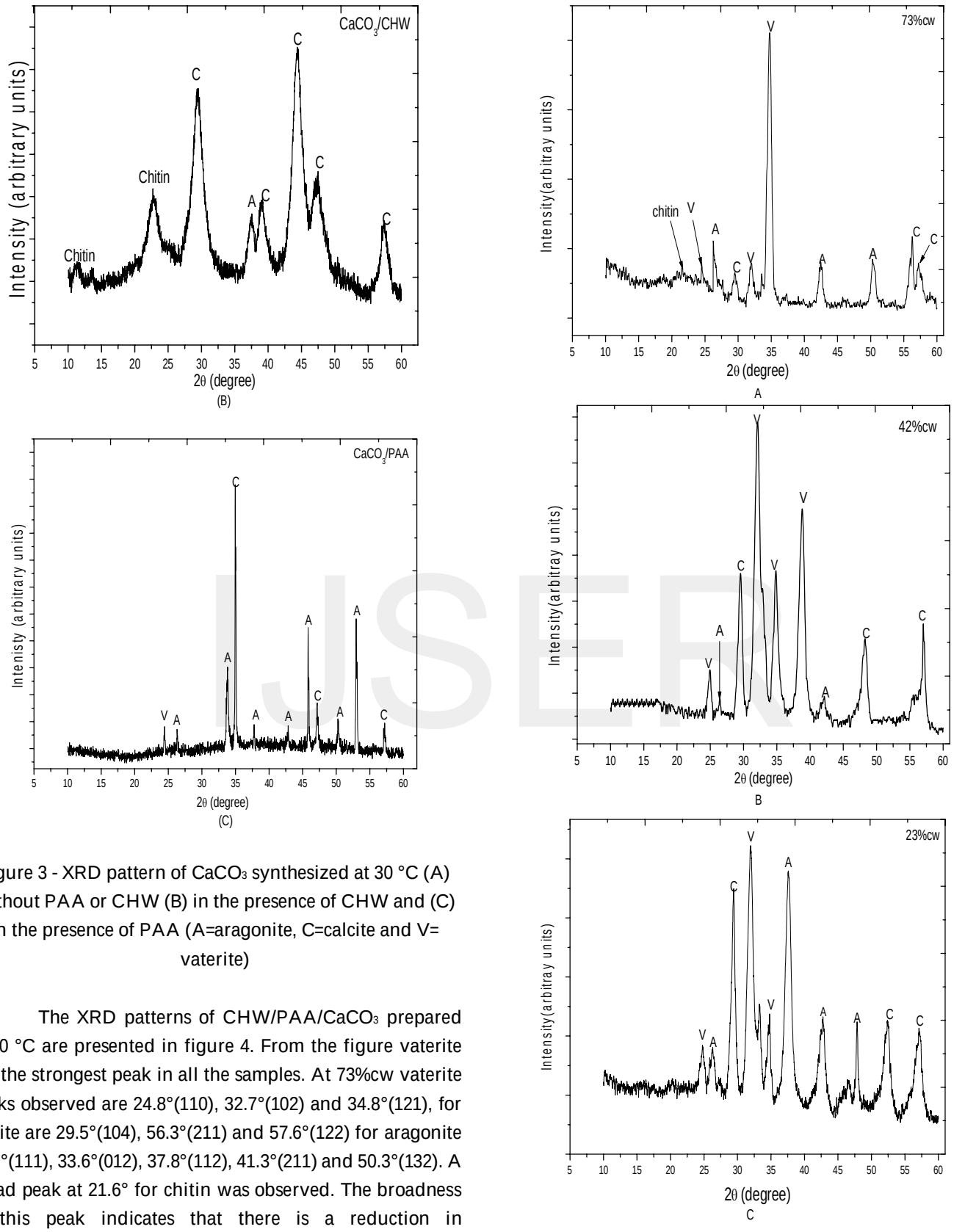

Figure 3 - XRD pattern of $CaCO_3$ synthesized at 30 °C (A) without PAA or CHW (B) in the presence of CHW and (C) in the presence of PAA (A=aragonite, C=calcite and V= vaterite)

The XRD patterns of CHW/PAA/$CaCO_3$ prepared at 30 °C are presented in figure 4. From the figure vaterite has the strongest peak in all the samples. At 73%cw vaterite peaks observed are 24.8°(110), 32.7°(102) and 34.8°(121), for calcite are 29.5°(104), 56.3°(211) and 57.6°(122) for aragonite 26.3°(111), 33.6°(012), 37.8°(112), 41.3°(211) and 50.3°(132). A broad peak at 21.6° for chitin was observed. The broadness of this peak indicates that there is a reduction in crystallinity of chitin. Other peaks for the various polymorphs are presented in table 1

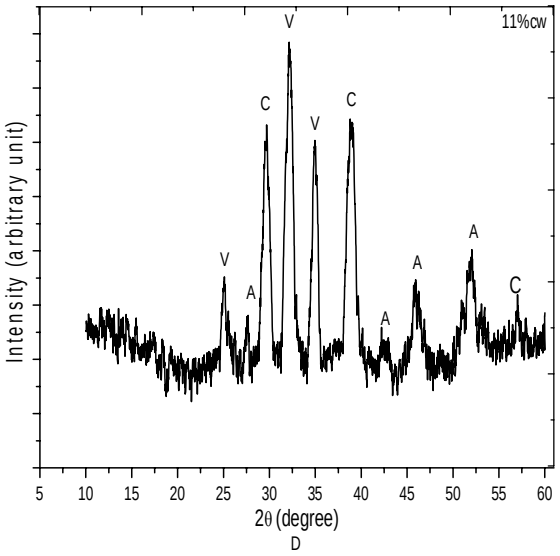

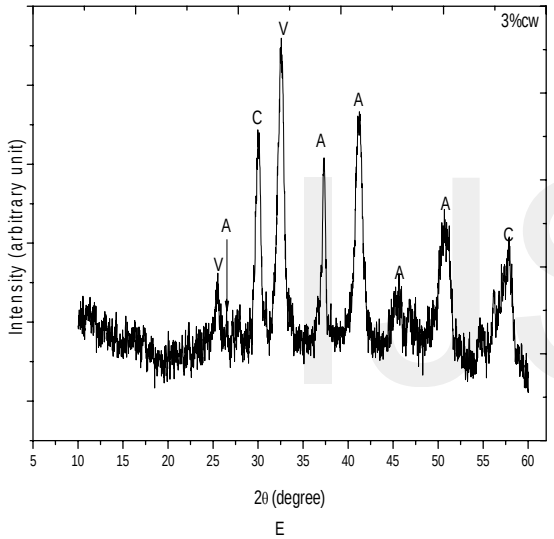

Figure 4 - XRD pattern of $CaCO_3$ synthesized at 30 °C in the presence of PAA (A) 72%cw,(B) 42%cw, (C) 23%cw, (D) 11%cw and (E) 3%c

Table1 - $CaCO_3$ polymorphs in the presence of PAA at different % chitin whiskers. A=aragonite, C= calcite and V= vaterite

73%cw	42%cw	23%cw	11%cw	3%cw	
2θ	2θ	2θ	2θ	2θ	Polymorph
21.6	-	-	-	-	Chitin
24.8	24.9	24.8	25.1	24.9	V
26.3	26.4	26.3	26.4	26.5	A
29.5	29.6	29.4	29.7	29.9	C
32.7	32.6	32.6	32.5	32.6	V
34.8	34.8	34.9	34.6	-	V
37.8	-	37.8	-	37.9	A
-	38.8	-	39.5	-	V
41.3	42.9	41.3	41.2	41.2	A
-	-	-	45.9	45.8	A
-	48.3	47.9	-	-	C
50.3	-	-	-	50.4	A
-	-	52.4	52.3	-	A
56.3	-	-	-	-	C
57.6	57.5	57.4	-	57.5	C
34.8	34.8	34.9	34.6	-	V

Rao [15], [24] established equations in which the fraction of calcite and vaterite can be determined. These equations are;

$$f_C = \frac{I_{104(c)}}{I_{110(v)} + I_{112(v)} + I_{104(c)} + I_{114(v)}} \quad 1$$

$$f_V = \frac{I_{110(v)} + I_{112(v)} + I_{114(v)}}{I_{110(v)} + I_{112(v)} + I_{104(c)} + I_{114(v)}} \quad 2$$

Where f_C and f_V are the calcite and vaterite fractions respectively , $I_{104(c)}$,$I_{110(v)}$,$I_{112(v)}$ and $I_{114(v)}$ are respectively the intensity at the reflection peaks at 104 for calcite, 110, 112 and 114 for vaterite. A modified X-ray calibration [25], line for the determination of molar fraction for the various compositions was also applied here. The equations are;

$$f_A = \frac{3.157x\, I_A^{111}}{I_C^{104} + 3.157\, x\, I_A^{111} + 7.691\, x\, I_V^{110}} \quad 3$$

$$f_C = \frac{f_A\, x\, I_C^{104}}{3.157\, x\, I_A^{111}} \quad 4$$

$$f_V = 1 - f_C - f_A \quad 5$$

Where f_A, f_C and f_V are respectively the fractions of aragonite, calcite and vaterite. I_A^{111} , I_C^{104} and I_V^{110} and are the intensity of aragonite, calcite and vaterite at the indicated planes respectively. Combining these five equations the molar fraction for calcite and other polymorph are presented in table 2.

Table 2 - Calcite (f_C) and vaterite (f_V) fractions based on the Rao equations and aragonite (f_A), calcite (f_c), and vaterite (f_V) fractions based on the Kontoyannis and Vagenas, equations.

	Kontoyannis and Vagenas, equations			Rao equations	
	f_A	f_C	f_V	f_C	f_V
$CaCO_3$	0.10	0.65	0.25	0.77	0.23
$CaCO_3$/CHW	0.30	0.20	0.50	0.62	0.38
$CaCO_3$/PAA	0.38	0.09	0.53	0.29	0.71
73%cw	0.10	0.22	0.68	0.31	0.69
42%cw	0.12	0.23	0.65	0.40	0.60
23%cw	0.13	0.23	0.64	0.50	0.50
11%cw	0.19	0.19	0.62	0.44	0.56
3%cw	0.26	0.13	0.61	0.18	0.82

From table 2 it can be seen that the calcite fraction using the Rao equation is 0.77 while the Kontoyannis and Vagenas equations yielded 0.65. The difference in fraction can be attributed to the fact that Rao is meant for a binary mixture of $CaCO_3$ crystallisation. The growth fraction of calcite in the absence of additive has been reported to be between 0.71 and 0.98 [6], [26]. Calcite is the thermodynamically most stable polymorph of $CaCO_3$ under ambient conditions but can convert to vaterite or aragonite when the degree of supersaturation is increased in the presence of a soluble or insoluble additive [26]. Cai *et al.,* [28] suggested a three stage mechanism of crystallisation; the formation of an unstable phase, the transformation of the unstable phase to a metastable phase and the development of the stable phase. Choi and Kuroda, [15] abridged these three stages to two; rapid crystallisation of amorphous calcium carbonate (ACC) to vaterite and the transformation of vaterite into calcite. The transformation rate according to Rodrigues-Blanco *et al.,* [29] is 10 times slower than the crystallisation step.

In the absence of CHW and PAA a binary mixture of vaterite and calcite was revealed by both Raman and XRD spectra confirming the low aragonite fraction as presented in table 2. In the presence of either PAA or CHW or both, a ternary mixture of $CaCO_3$ consisting of calcite, vaterite and aragonite with a gradual decrease of calcite and vaterite in favour of aragonite as CHW decreases. The presence of amorphous calcium carbonate (ACC) in the Raman spectra at 1461 cm^{-1} and the high vaterite fraction in all samples (except the one without additives or CHW) points to the fact that ACC and indeed vaterite can be stabilised in the presence of PAA and CHW. This is an indication that the rate of the first step, that is, the formation of an unstable phase is slower in the presence of PAA and CHW, making the second step a non determining stage for the rate of crystallisation (from ACC to calcite via vaterite or ACC to calcite depending on the stages). In other words, the high vaterite fraction points to the fact that the conversion of vaterite to calcite via the metastable aragonite as PAA increases was slow and incomplete. Due to the incomplete conversion, all three polymorph were observed.

The high vaterite fraction can equally be discussed in relation to the molecular weight of PAA. Using the Kontoyannis and Vagenas equations, the growth of $CaCO_3$ crystals in the presence of CHW reduced calcite growth from 0.65 to 0.20 while the calcite growth fractions in the presence of PAA reduces to 0.09. The reduction in the fractional growth of calcite in the presence of PAA and CHW indicates that both polymers may be acting as inhibitors. Tang *et al.,* [26] has shown that PAA can act as inhibitor. The higher the concentration, the slower the precipitate of $CaCO_3$. Based on the decrease of the grain size of calcite Kotachi *et al.,* [29] reported that the inhibition strength of PAA increases with increase in molecular weight. Huang *et al.,* [27] reported that at higher molecular weight of PAA-Na (M_w=250,000), the obtained vaterite $CaCO_3$ crystals were stable with a high yield of between 69 and 82% irrespective of the concentration ratios and the delayed (addition of sodium salts at different time) addition time. At lower molecular weight, the vaterite obtained under lower concentration ratio transformed to calcite for an incubation period of 5 days with a high yield of 88 %. This remained stable at high concentration with low yield of 44 %. Fantinel *et al.,* [31] reported an increasing binding strength between PAA-Na and Ca^{2+} as the molecular weight increased. The increase was due to the bichelating mechanism and increased torsion in the longer polyelectrolyte chains [21]. At higher molecular weight, PAA-Na exhibit stronger binding strength on the surfaces of the vaterite particles than at lower molecular weight. The strong binding strength at higher molecular weight may help in stabilising the vaterite particles. Based on the above the high volume fraction obtained here at different filler loading can equally be attributed to the high molecular weight of the PAA used.

3.3 Scanning Electron Microscopy Morphology

Figure 5 shows the SEM images of $CaCO_3$ precipitate synthesized at 30 °C without PAA at (A) low and (B) high magnifications. From the figure it can be seen that rhombohedral calcite with traces of vaterite (Figure 5B arrow pointing) $CaCO_3$ polymorphs were formed. The calcite exhibits regular and step like smooth faces and has an average edge of 1.4 µm. The shape of the rhombohedral calcite seems to be similar. Similarities in calcite structure were reported in the literature [6], [27], [32]. Depending on the pH value, Shivkumara *et al.,* [32] obtained a mixture of calcite and vaterite when the pH value was ~5, but only calcite was observed when the pH was between 7-7.5 No precipitate of $CaCO_3$ was observed outside this range. Ouhenia *et al.,* [6] obtained a mixture of calcite and vaterite although the pH value was not stated.

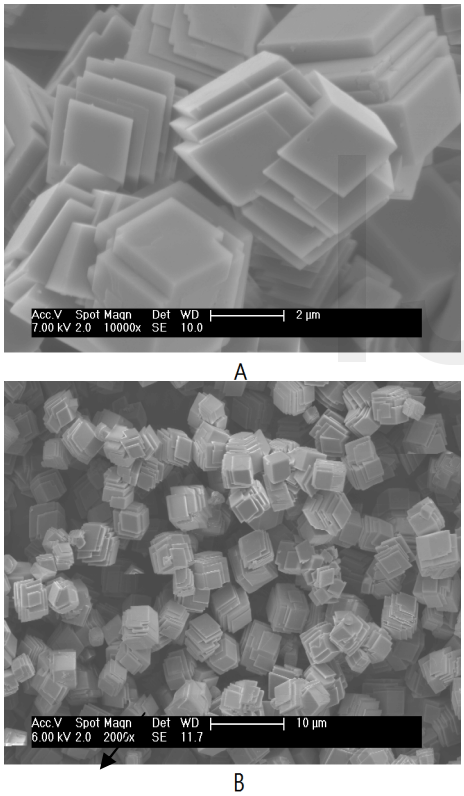

Figure 5- SEM images of $CaCO_3$ particles synthesized at 30 °C without PAA incorporation. (A) high and (b) low magnification images of rhombohedral calcite (arrow pointing at traces of spherical vaterite)

Figure 6A is SEM image of $CaCO_3$ in the presence of PAA showing clearly two different morphologies. Aragonite rods of $CaCO_3$ of about 50 nm in diameter are observed which are aligned parallel to each other. Another feature of $CaCO_3$/PAA is the exhibition of clusters of grains or spherical lump (insert picture with arrow) of vaterite. Spherical vaterite has been obtained when G0.5 poly(amidoamine)(PAMAM) dendrimer was used to study the influence of incubation time of dendrimer $CaCl_2$ solution on the formation of calcium carbonate[33]. Figure 6B presents the SEM image of calcium carbonate crystallization in the presence of CHW.

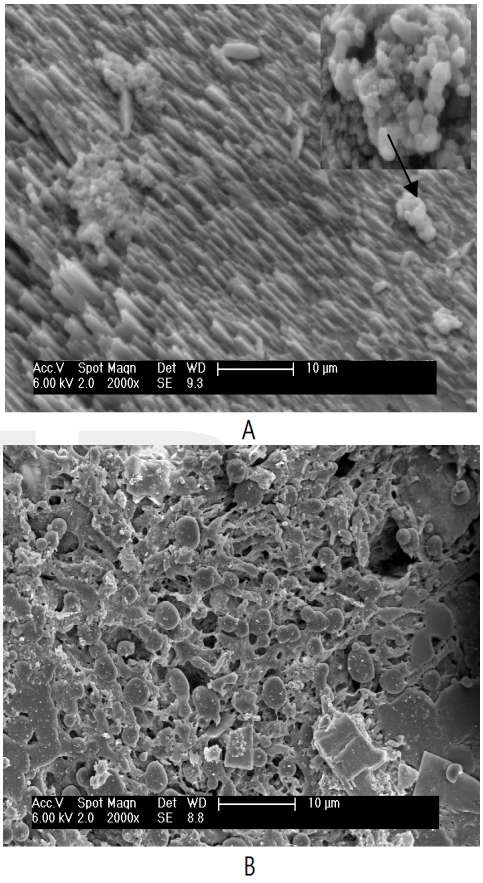

Figure 6 - SEM images of $CaCO_3$ particles synthesized at 30 °C in the presence of (A) PAA (arrow pointing at clusters of spherical lump of vaterite) and (B) CHW.

Contrary to the normal rhombohedral calcite, calcium carbonate crystallization in the presence of CHW has a morphological mixture of ellipsoidal and disc shape crystals and smaller aggregate of rhombohedral calcite. Figure 7 presents calcium carbonate crystallization in the presence of PAA at different filler loading of CHW. The SEM images show a mixture of rhombohedral calcite and spherical vaterite. As CHW content reduces the rhombohedral shape shows roughness and less regular

faces making it difficult to measure the face size. Ouhenia *et al.,* [6] attributed such roughness to the decrease in Ca^{2+} free ions in the solution due to the formation of polyelectrolyte complexes. Similar rough cubic particles with uneven surfaces of calcite in the presence of PAA have been reported [34]. The vaterite particles form agglomerates in all the samples although there are some particles which do not join the agglomerates. The vaterite size at 3 %cw loading was between 3 to 24.8 µm porosities which were equally observed.

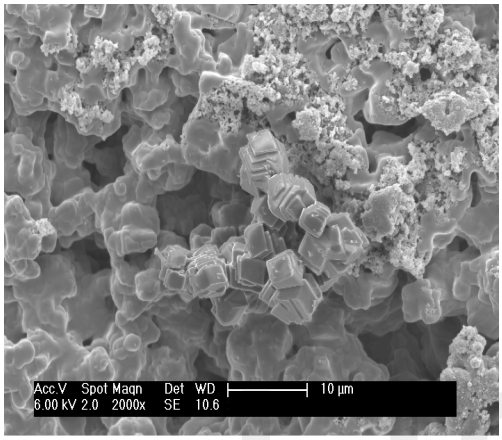

A

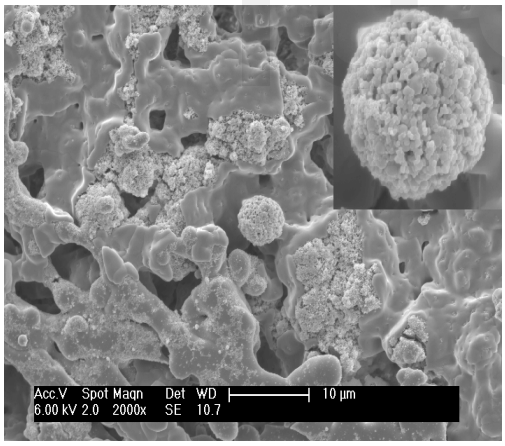

B

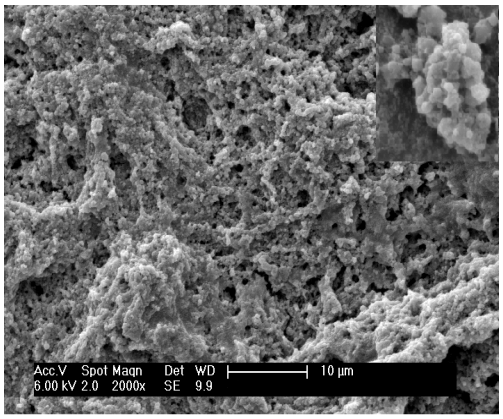

C

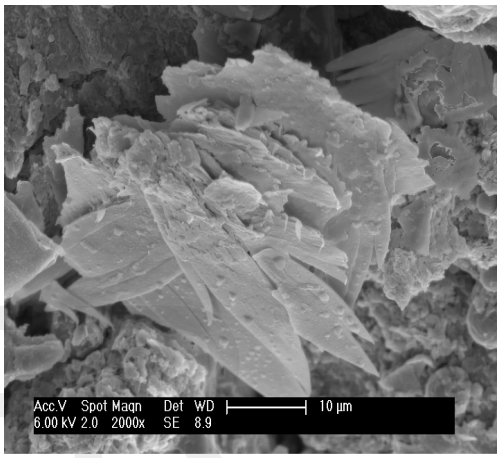

D

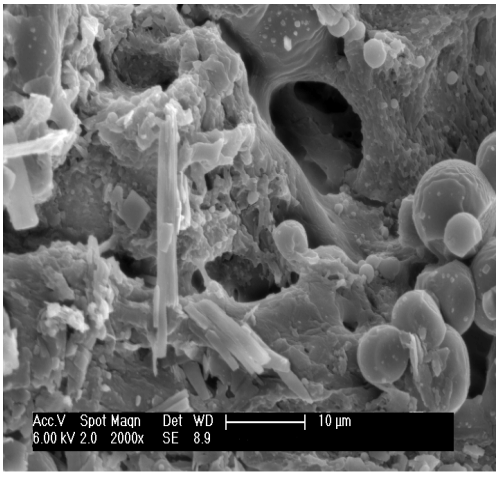

E

Figure 7- SEM images of $CaCO_3$ particles synthesized at 30 °C in the presence of PAA (A) 73%cw, (B)42%cw, (C) 23%cw, (D)11%cw and (E) 3%cw at different filler loading of CHW.

Conclusion

A solution and evaporation casting method (as against the common vapour diffusion method) was used to induce $CaCO_3$ crystal growth using CHW and PAA as templates. Rhombohedral calcite was observed in the absence of PAA and CHW. Rods like aragonite polymorph were seen when PAA alone was used as a template together with clusters of spherical vaterite. A morphological mixture of ellipsoidal and disc shape crystals with traces of rhombohedral aggregate calcite were the features of $CaCO_3$ crystallization in the presence of CHW. When both PAA and CHW were used as templates, the rhombohedral shape of calcite showed roughness with irregular faces while the vaterite particles continue to agglomerate with the observations of porosities at higher filler loading. There was a gradual decrease in vaterite fraction as CHW decreases while PAA increases. At lower CHW content, aragonite polymorph growth was favoured to the detriment of the calcite. It has also been shown that$CaCO_3$ can be grown in the presence of soluble and insoluble additive (PAA and CHW) within a very short time (5 minutes at 30° C) employing the evaporation method. The results also show that the vaterite polymorph can be grown even at higher filler loadings.

References

[1]. N. Hosoda and T. Kato, "Thin-Film Formation of Calcium Carbonate Crystals: Effects of Functional Groups of Matrix Polymers" Chemistry of Materials, vol. 13, pp. 688-693, 2001.

[2]. Y. Yamamoto, T. Nishimura, T. Saito and T. Kato, "CaCO3/chitin-whisker hybrids: formation of $CaCO_3$ crystals in chitin-based liquid-crystalline suspension" Polymer Journal, vol. 42, pp. 583-596, 2010.

[3]. A. Kotachi, T. Miura and H. Imai, "Polymorph Control of Calcium Carbonate Films in a Poly (acrylic acid)-Chitosan System" Crystal Growth and Design, vol. 6, pp.1636-1641, 2006

[4]. N.H. Munro and K McGrath, "How important is polyelectrolyte complex formation in biomimetic mineralisation manipulation via alcohol addition" Dalton Transaction, vol. 42, pp.8259-8269, 2013.

[5]. A. Sugawara, T. Ishii and T. Kato, "Self-Organized Calcium Carbonate with Regular Surface-Relief Structures" Angewandte Chemie International Edition, vol. 42, pp.5299-5303, 2003.

[6]. S. Ouheniaa, D. Chateigner, M. Belkhira, E. Guilmeaub and C. Kraussb, "Synthesis of calcium carbonate polymorphs in the presence of polyacrylic acid" Crystal growth, vol. 310, pp.2832-2841, 2008.

[7]. T. Nishimura, T. Ito, Y. Yamamoto, M. Yoshio and T. Kato, "Macroscopically Ordered Polymer/CaCO3 Hybrids Prepared by Using a Liquid-Crystalline Template" Angewandte Chemie International Edition, vol. 47, pp.2800-2803, 2008.

[8]. J. Junkasem, R. Rujiravanit and P. Supaphol, "Fabrication of α-Chitin Whisker Reinforced Poly(vinylalcohol) Nanocomposite Nanofibers by Electrospinning" Nanotechnology, vol. 17, pp.4519-4528, 2006.

[9]. J. Junkasem, R. Rujiravanit, B.P. Grady and P. Supaphol, "X-Ray Diffraction and Dynamic Mechanical Analyses of α-Chitin Whisker-Reinforced Poly (vinyl alcohol) Nanocomposite Nanofibers. Polymer International, vol. 59, pp.85-91,2010.

[10]. A. Morin and A. Dufresne, "Nanocomposites of Chitin Whiskers from Riftia Tubes and Poly (caprolactone)" Macromolecules, vol. 35, pp.2190-2199, 2002.

[11]. D. Chakrabarty and S. Mahapatra, "Aragonite crystals with unconventional morphologies. J. Material Chemistry, vol. 9, pp.2953-2957, 1999.

[12]. U. Wehrmeister, A. L. Soldati, D.E. Jacob, T. Häger, and W. Hofmeister, "Raman spectroscopy of synthetic, geological and biological vaterite: a Raman spectroscopic Study" J. Raman Spectroscopy, vol. 41, pp.193-201, 2010.

[13]. N.H. Munro and K. McGrath, "How important is polyelectrolyte complex formation in biomimetic mineralisation manipulation via alcohol addition" Dalton Transaction, vol. 42, pp. 8259-8269, 2013.

[14]. S. Gunasekaran, G. Anbalagan and S. Pandi, "Raman and infrared spectra of carbonates of calcite structure" J. Raman Spectroscopy, vol. 37, pp.892-899, 2006.

[15]. K. Choi and k. Kuroda, "Polymorph Control of Calcium Carbonate on the Surface of Mesoporous

Silica" Crystal Growth and Design, vol. 12, pp.887-893, 2012.

[16]. M. Ofem, "Properties of chitin whisker reinforced poly(acrylic acid) composites, PhD Thesis, School of Materials, The University of Manchester, 2015.

[17]. E. Dalas and P.G. Koutsoukos, "The crystallization of vaterite on cholesterol. J. Colloidal Interface Science, vol. 127, pp.273-280, 1989.

[18]. L. He, R. Xue and R. Song, "Formation of calcium carbonate films on chitosan substrates in the presence of poly(acrylic acid)" J. Solid State Chemistry, vol. 182, pp.1082-1087, 2009.

[19]. N. Wada, S. Suda, K. Kanamura and T. Umegaki, "Formation of thin calcium carbonate films with aragonite and vaterite forms coexisting with poly (acrylic acids) and chitosan membranes. J. Colloidal Interface Science, vol. 277, pp.167-174, 2004.

[20] I. Martinez, J. Zhang and R.J. Reeder, "In situ X-ray diffraction of aragonite and dolomite at high pressure and high temperature; evidence for dolomite breakdown to aragonite and magnesite" American Mineralogist, vol. 81, pp.611-624, 1996.

[21]. S.P. Gopi and V.K. Subramanian, "Polymorphism in $CaCO_3$ - Effect of temperature under the influence of EDTA (di sodium salt,)" Desalination vol. 297, pp.38-47, 2012.

[22] C, Lin, C. Lee and W. Chiu, "Preparation and properties of poly(acrylic acid) oligomer stabilized superparamagnetic ferrofluid" J. Colloid and interface Science, vol. 291, pp.411-420, 2005.

[23]. S. Chen and H. Lee, "Structure and properties of Poly(acrylic acid)-Doped Polyaniline" Macromolecules, vol. 28: , pp.2858-2866, 1995.

[24]. M.S. Rao, "Kinetics and Mechanism of transformation of Vaterite to calcite" Bulletin of the Chemical Society of Japan, vol. 46, pp.1414-1417, 1973.

[25]. C. G. Kontoyannis and N.V. Vagenas, "Calcium carbonate phase analysis using XRD and FT-Raman Spectroscopy" Analyst, vol.125, pp.251-255, 2000.

[26]. Y. Tang, W. Yang, X. Yin, Y. Liu, P. Yin and J. Wang, "Investigation of $CaCO_3$ scale inhibition by PAA, ATMP and PAPEMP" Desalination, vol. 228, pp.55-60, 2008.

[27]. S. Huang, K. Naka and Y. Chuj, "Effect of molecular weights of poly(acrylic acid) on crystallization of calcium carbonate by delayed addition method" Polymer Journal, vol. 40, pp.154-162, 2008.

[28]. Z.G. Cai, G.J. Jiang, S. M. Qin, P.B. Lin, M. Tao and S.Z. Zheng, "Investigation of scale inhibition mechanisms based on the effect of scale inhibitor on calcium carbonate crystal forms" Science in China B: Chemistry, vol. 50, pp.114-120, 2007.

[29]. J.D. Rodriguez-Blanco, S. Shaw and L.G. Benning, "The kinetics and mechanisms of amorphous calcium carbonate (ACC) crystallization to calcite, via vaterite" Nanoscale, vol. 3, pp.265-271, 2011.

[30]. A, Kotachi, T. Miura and Imai H, "Morphological Evaluation and Film Formation with Iso-Oriented Calcite Crystals Using Binary poly (acrylic acid)" Chemistry of Materials, vol. 16, pp.3191-3196, 2004.

[31]. F. Fantinel, J. Rieger, F. Molnar and P. Hübler, "Complexation of Polyacrylates by Ca^{2+} Ions. Time-Resolved Studies Using Attenuated Total Reflectance Fourier Transform Infrared Dialysis Spectroscopy" Langmuir, vol. 20, pp.2539-2543, 2004.

[32]. C. Shivkumara, P. Singh, A. Gupta and M.S. Hegde, "Synthesis of vaterite $CaCO_3$ by direct precipitation using glycine and L-alanine as directing agents" Materials Research Bulletin, vol. 41, pp.1455-1460, 2006.

[33]. Y. Tanaka and K. Naka, "A carbonate controlled-addition method for size-controlled calcium carbonate spheres by carboxylic acid-terminated poly (amidoamine) dendrimers. Polymer Journal, vol. 42, pp.676-683, 2010.

[34]. Y. Pan, X. Zhao, Y. Guo, X. Lv, S. Ren, M. Yuan and Z. Wang, "Controlled synthesis of hollow calcite microspheres modulated by polyacrylic acid and sodium dodecyl sulfonate" Material Letters, vol. 61, pp.2810-2813, 2007.

ISSN 2229-5518
Authors:
Michael Ikpi Ofem (PhD), Department of Mechanical Engineering Cross River University of Technology Calabar, Nigeria
Muneer Umar (PhD), Department of Chemical Engineering Federal Polytechnic Nasarawa Nigeria
Musa Muhammed (M.Eng), Department of Mechanical Engineering Federal Polytechnic Nasarawa Nigeria